A Comparison of Fuzzy Schemes for Trajectory Tracking on the Furuta Pendulum*

Astolfo Coronado * Ollin Peñaloza-Mejía *
Victor Estrada-Manzo * Miguel Bernal *

* *Department of Electrical and Electronics Engineering, Sonora Institute of Technology, Ciudad Obregón, Mexico*
e-mail: miguel.bernal@itson.edu.mx

Abstract: This paper presents real-time implementation of trajectory tracking on a Furuta pendulum via two fuzzy output regulation schemes: the first one uses convex representations; the second one employs dynamic mappings. Additionally, the stabilizing part of the control law is computed by means of linear matrix inequalities, so speed convergence and input constraints can be directly considered. Simulation and real-time results are given to show the effectiveness of the approaches.

Keywords: Trajectory tracking; output regulation; fuzzy mappings; dynamic mapping; fuzzy modeling; Furuta pendulum.

1. INTRODUCTION

Tracking a reference is a common task in control systems; it can be performed via the output regulation theory, both for linear systems (Francis, 1977) and nonlinear ones (Isidori and Byrnes, 1990). This problem is solvable if and only if a set of nonlinear partial differential equations –better known as the Francis-Isidori-Byrnes (FIB) ones– has a solution (Isidori, 1995). These sort of equations are, except in simple cases, very hard to solve analytically.

The output regulation problem consists in finding a control law such that the tracking error tends asymptotically to zero; this error signal depends on the system outputs and some trajectories derived from a neutrally stable exosystem (Isidori, 1995), i.e., broadly speaking, a system that generates periodic or quasi-periodic trajectories. Output regulation provides necessary and sufficient conditions, but, as mentioned above, requires solving the FIB equations, which might be impossible to do. In order to cope with nonlinear output regulation, different methodologies have been proposed: fuzzy ones (Begovich et al., 2002; Meda and Castillo, 2009), using linear matrix inequalities (LMIs) altogether with exact convex models (Bernal et al., 2012), and computing dynamic mappings (Meda et al., 2012; Robles and Bernal, 2015).

Based on the above, this paper compares two fuzzy nonlinear methodologies to perform trajectory tracking:

(1) Via an exact convex representation, based on which a local regulator is designed for each vertex linear system; the global control law being a convex interpolation of the local controllers (Meda and Castillo, 2009).
(2) Via dynamic output regulation, which does not solve the FIB equations, but dynamically incorporate them into the closed-loop scheme (Meda et al., 2012; Robles and Bernal, 2015).

Importantly, the methodologies above are implemented assuming that the state is fully available and that the fuzzy rule-based system is uniformly distributed in the state space to cover the region of interest. These are some of the reasons behind our choice of the Furuta pendulum as the plant where the schemes above are implemented; the others being its highly nonlinear nature and the inherent difficulty of its underactuated nature (Fantoni and Lozano, 2002).

This paper is organized as follows: the next section introduces the reader to the Furuta pendulum where real-time implementations are later performed; section 3 constructs a fuzzy model –better known as a Takagi-Sugeno (TS) one– for the Furuta pendulum: it will be important for LMI stabilization purposes; section 4 briefly presents the output regulation schemes trajectory tracking is based on: fuzzy and dynamic; simulation and real-time results are given in section 5; this report concludes in section 6 with some final remarks.

2. THE FURUTA PENDULUM

In Fig. 1, a Furuta pendulum mechanism manufactured by Quanser is shown; it consists of two joint beams: an horizontal one which rotates thanks to a DC motor and a vertical one which is fixed to one end of the first one and freely rotates. The system is underactuated (Quanser, 2006).

* This work has been supported by the PROFAPI Project 2017-0088 and the Mexican Council of Science and Technology (CONACYT) through scholarship 449890 and postdoctoral fellowship CVU 366627.

The dynamics of the Furuta pendulum are computed by means of the Lagrange-Euler methodology, which yields the following set of differential equations (arguments will be omitted where they can be inferred by the context):

$$0 = c_2 \sin^2\theta + c_1\ddot{\phi} + c_4\cos\theta\ddot{\theta} + 2c_2\dot{\phi}\dot{\theta}\cos\theta\sin\theta - c_4\dot{\theta}^2\sin\theta - u(t) \tag{1}$$
$$0 = c_4\cos\theta\ddot{\phi} + (c_2+c_3)\ddot{\theta} - c_5 g\sin\theta - c_2\dot{\phi}^2\cos\theta\sin\theta$$

where ϕ is the angle of the horizontal beam, θ is the angle between vertical beam and the upright position, and $u(t)$ is control input. The parameters of the plant are: $c_1 = 0.0363$, $c_2 = 0.0306$, $c_3 = 0.356$, $c_4 = 0.0260$, $c_5 = 0.3829$, and the gravity acceleration $g = 9.81\mathrm{m/s}^2$.

For our control purposes, a state-space representation $\dot{x}(t) = f(x(t), u(t))$ of the system is required; it is obtained from (1) by choosing the state variables as $x_1(t) = \phi$, $x_2(t) = \dot{\phi}$, $x_3(t) = \theta$, and $x_4(t) = \dot{\theta}$, i.e.:

$$\underbrace{\begin{bmatrix}\dot{x}_1\\ \dot{x}_2\\ \dot{x}_3\\ \dot{x}_4\end{bmatrix}}_{\dot{x}} = \underbrace{\begin{bmatrix}0 & 1 & 0 & 0\\ 0 & 0 & (\eta_1-\eta_2)\eta_5 & 0\\ 0 & 0 & 0 & 1\\ 0 & 0 & (\eta_3-\eta_4)\eta_5 & 0\end{bmatrix}}_{A(x)} \underbrace{\begin{bmatrix}x_1\\ x_2\\ x_3\\ x_4\end{bmatrix}}_{x} + \underbrace{\begin{bmatrix}0\\ -(c_2+c_3)\eta_5\\ 0\\ c_4\cos x_3\eta_5\end{bmatrix}}_{B(x)} u, \tag{2}$$

where

$$\eta_1 = c_4\cos x_3\left(c_2 x_2^2\cos x_3 + gc_5\right)\sin x_3/x_3,$$
$$\eta_2 = (c_2+c_3)(c_4 x_4^2 - 2c_2x_2x_4\cos x_3)\sin x_3/x_3,$$
$$\eta_3 = c_4\cos x_3(c_4 x_4^2 - 2c_2x_2x_4\cos x_3)\sin x_3/x_3,$$
$$\eta_4 = (c_2\sin^2 x_3 + c_1)(c_2x_2^2\cos x_3 + gc_5)\sin x_3/x_3,$$
$$\eta_5 = c_4^2\cos^2 x_3 - (c_2+c_3)(c_2\sin^2 x_3 + c_1).$$

where $\lim_{x_3\to 0}\sin x_3/x_3 = 1$. This model will be employed for further developments.

3. A FUZZY MODEL OF THE FURUTA PENDULUM

Constructing a fuzzy TS system of (2) can be done by means of the sector nonlinearity approach (Taniguchi et al., 2001). To that end, consider the compact set $\Omega = \{|x_2| \le 10(rad/s), |x_3| \le 0.3(rad), |x_4| \le 3(rad/s)\}$; then, one can identify 4 bounded non-constant terms $z_l(x) \in \left[z_l^0, z_l^1\right]$, $l \in \{1,2,3,4\}$ in matrices $A(x)$ and $B(x)$; the non-constant terms and their bounds are given in Table 1.

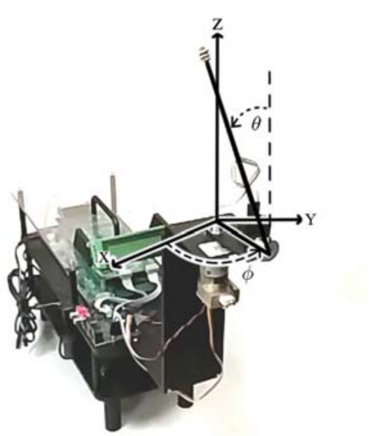

Fig. 1. Scheme of the Furuta pendulum.

Table 1. Non-constant terms in (2) and their bounds

Term	Definition	Lower bounds z_l^0	Upper bounds z_l^1
$z_1(x)$	$\eta_1 - \eta_2$	0.0875	0.0976
$z_2(x)$	$\eta_3 - \eta 4$	−0.1497	−0.1363
$z_3(x)$	η_5	−579.0186	−467.9967
$z_4(x)$	$c_4\cos x_3$	$-c_4$	c_4

Each of the nonlinear terms $z_l(x)$ can be expressed as a convex sum of its bounds in the compact set Ω:

$$z_l(x) = \underbrace{\frac{z_l^1 - z_l(x)}{z_l^1 - z_l^0}}_{w_0^l(x)}\left(z_l^0\right) + \underbrace{\frac{z_l(x) - z_l^0}{z_l^1 - z_l^0}}_{w_1^l(x)}\left(z_l^1\right) = \sum_{l_j=0}^{1} w_{l_j}^l(x) z_l^{l_j},$$

where the scalar functions $w_{l_j}^l(x)$, $l_j \in \{0,1\}$ hold the convex-sum property in Ω, that is, $w_{l_j}^l(x) \in [0,1]$ and $w_0^l(x) + w_1^l(x) = 1$. Since convex sums can be stacked together, the model (2) is algebraically equivalent to:

$$\dot{x} = \sum_{l_1=0}^{1}\sum_{l_2=0}^{1}\sum_{l_3=0}^{1}\sum_{l_4=0}^{1} w_{l_1}^1(x)w_{l_2}^2(x)w_{l_3}^3(x)w_{l_4}^4(x) \times\left(\underbrace{\begin{bmatrix}0 & 1 & 0 & 0\\ 0 & 0 & z_1^{l_1}z_3^{l_3} & 0\\ 0 & 0 & 0 & 1\\ 0 & 0 & z_2^{l_2}z_3^{l_3} & 0\end{bmatrix}}_{A_i} x + \underbrace{\begin{bmatrix}0\\ -(c_2+c_3)z_3^{l_3}\\ 0\\ z_3^{l_3}z_4^{l_4}\end{bmatrix}}_{B_i} u\right)$$
$$= \sum_{i=1}^{16} h_i(x)\left(A_i x + B_i u\right), \tag{3}$$

where $h_i(x) = w_{l_1}^1(x)w_{l_2}^2(x)w_{l_3}^3(x)w_{l_4}^4(x)$, $[l_1 l_2 l_3 l_4]$ is the 4-digit binary representation of $(l-1)$, $i \in \{1, 2, \ldots, 16\}$. For instance, $h_7(x) = w_0^1(x)w_1^2(x)w_1^3(x)w_0^4(x)$ leads to the following linear matrices:

$$A_7 = \begin{bmatrix}0 & 1 & 0 & 0\\ 0 & 0 & z_1^0 z_3^1 & 0\\ 0 & 0 & 0 & 1\\ 0 & 0 & z_2^1 z_3^1 & 0\end{bmatrix}, B_7 = \begin{bmatrix}0\\ -(c_2+c_3)z_3^1\\ 0\\ z_3^1 z_4^0\end{bmatrix}.$$

Due to space reasons, only some of the computed matrices A_i, B_i are given below:

$$A_1 = \begin{bmatrix}0 & 1 & 0 & 0\\ 0 & 0 & -17.9042 & 0\\ 0 & 0 & 0 & 1\\ 0 & 0 & 170.0130 & 0\end{bmatrix}, A_5 = \begin{bmatrix}0 & 1 & 0 & 0\\ 0 & 0 & -17.9042 & 0\\ 0 & 0 & 0 & 1\\ 0 & 0 & 72.4582 & 0\end{bmatrix},$$

$$A_{11} = \begin{bmatrix}0 & 1 & 0 & 0\\ 0 & 0 & -144.3065 & 0\\ 0 & 0 & 0 & 1\\ 0 & 0 & 149.5780 & 0\end{bmatrix}, A_{15} = \begin{bmatrix}0 & 1 & 0 & 0\\ 0 & 0 & -144.3065 & 0\\ 0 & 0 & 0 & 1\\ 0 & 0 & 63.7487 & 0\end{bmatrix},$$

$$B_1 = B_5 = \begin{bmatrix}0\\ 38.3310\\ 0\\ -14.3820\end{bmatrix}, B_{11} = B_{15} = \begin{bmatrix}0\\ 33.7237\\ 0\\ -12.6534\end{bmatrix}.$$

Note that the fuzzy TS system (3) can be viewed as an interpolation of linear systems, where the interpolating functions $h_i(x)$, $i \in \{1, 2, \ldots, 16\}$, "captured" the system nonlinearities. Moreover, by construction, these functions hold the convex sum property $\sum_i h_i(x) = 1$, $h_i(x) \in [0, 1]$ in Ω.

4. TRAJECTORY TRACKING VIA OUTPUT REGULATION

Consider the nonlinear system:

$$\begin{aligned} \dot{x}(t) &= f(x) + g(x)u(t) \\ \dot{w}(t) &= s(w) \\ e(t) &= Cx(t) - Qw(t), \end{aligned} \tag{4}$$

where $x(t) \in X \subset \mathbb{R}^n$ is the state vector to be driven, $w(t) \in W \subset \mathbb{R}^q$ is the exosystem that provides the references, and $e(t) \in \mathbb{R}^p$ is the tracking error. For instance, if the tracked reference is a scalar term, $Cx(t)$ can be viewed as a scalar output which should follow $Qw(t)$ which is the exosystem output (reference).

Solving the nonlinear output regulation problem consists in finding a control law

$$u = \alpha(x, w), \tag{5}$$

such that $\lim_{t\to\infty} e(t) = 0$ for any initial condition $(x(0), w(0)) \in \Omega \subset X \times W$ as well as $\dot{x}(t) = f(x)x + g(x)\alpha(x, 0)$ has the origin $x = 0$ exponentially stable.

Then, the nonlinear output regulation problem has a solution if and only if (Isidori and Byrnes, 1990):

(1) $w = 0$ is a stable equilibrium point of $\dot{w} = S(w)$ and $\exists \tilde{W} \subset W \supset 0 : \forall w(0) \in \tilde{W}$ is Poisson-stable.
(2) $(f(x), g(x))$ has a controllable linear approximation in $x = 0$.
(3) If there exists mappings $x = \pi(w)$, $\pi(0) = 0$, and $u = \gamma(w)$, $\gamma(0) = 0$ defined in $W^0 \subset W$ including the origin, such that:

$$\frac{\partial \pi}{\partial w} s(w) = f(\pi(w)) + g(\pi(w))\gamma(w) \tag{6}$$

$$0 = C\pi(w) - Qw. \tag{7}$$

The control law is given by (5) with $\alpha(x, w) = \gamma(w) + K(x - \pi(w))$.

Solving the aforementioned nonlinear partial differential equations (6)-(7) is a difficult task (Meda et al., 2012). In this work two fuzzy methodologies are employed in order to avoid explicitly solving the partial differential equations:

(1) Via a fuzzy TS model of (2) we can solve local linear output regulation instances which will be later interpolated using the very same interpolating functions of the model (Meda and Castillo, 2009).
(2) Via a dynamic output regulation originally appeared in the fuzzy context in (Meda et al., 2012) and later corrected in (Robles and Bernal, 2015), which has the advantage of being less approximate than the first scheme, while leading to more involved expressions for the nonlinear mappings.

The next two subsections develop the methodologies just described for the Furuta pendulum.

4.1 Trajectory tracking via fuzzy output regulation

This section presents developments which lead to the output regulation via TS models. It is mainly based on the linear output regulation approach (Francis, 1977). Let us summarize it by considering the following linear system

$$\dot{x}(t) = Ax(t) + Bu(t), \tag{8}$$

$$\dot{w}(t) = Sw(t), \tag{9}$$

$$e(t) = Cx(t) - Qw(t), \tag{10}$$

where $x(t) \in X \subset \mathbb{R}^n$ is the state vector to be driven, $w(t) \in W \subset \mathbb{R}^q$ is the exosystem that provides the references, $e(t) \in \mathbb{R}^p$ the tracking error; $A \in \mathbb{R}^{n\times n}$, $B \in \mathbb{R}^{n\times m}$, $C \in \mathbb{R}^{p\times n}$, and $Q \in \mathbb{R}^{p\times q}$ are known constant matrices.

The output regulation problem consists in finding a control law

$$u(t) = Kx(t) + Lw(t), \quad K \in \mathbb{R}^{m\times n}, \quad L \in \mathbb{R}^{m\times q}, \tag{11}$$

such that $\lim_{t\to\infty} e(t) = 0$ for any initial condition $(x(0), w(0)) \in \Omega \subset X \times W$. In (Francis, 1977), it is proven that the output regulation problem has a solution if and only if

1. $Re\{\sigma(S)\} \geq 0$ (exosystem being neutrally stable).
2. (A, B) is stabilizable.
3. $\exists \Pi \in \mathbb{R}^{n\times q}$ and $\Gamma \in \mathbb{R}^{m\times q}$ such that:

$$\Pi S = A\Pi + B\Gamma, \quad 0 = C\Pi - Q. \tag{12}$$

Finally, control law (11) is built with K such that $A+BK$ is Hurwitz (computed by any method) and $L = \Gamma - K\Pi$.

Following the idea given in (Meda and Castillo, 2009), computing a nonlinear control law for the Furuta system (2) of the form

$$u = \sum_{i=1}^{16} h_i(x)\left(Kx + (\Gamma_i - K\Pi_i)w\right) \tag{13}$$

requires the fuzzy TS model (3) and finding 16 pairs of gains (Π_i, Γ_i), $i \in \{1, 2, \ldots, 16\}$ such that:

$$\Pi_i S = A_i \Pi_i + B_i \Gamma_i, \quad , 0 = C\Pi_i - Q, \tag{14}$$

for $i \in \{1, 2, \ldots, 16\}$. Thus, each vertex performs local regulation (Begovich et al., 2002).

One of the advantages of using fuzzy TS models is that stabilization conditions are cast as LMIs, this eases the incorporation of certain performances, such as: decay rate (or speed converge), input constraints, output constraints, etc. Since the goal of the paper is real-time implementation of nonlinear control laws, we propose to compute the gain K in (13) by means of the following LMIs:

$$A_i X + B_i M + XA_i^T + M^T B_i^T + 2\alpha X < 0, \; X > 0, \tag{15}$$

$$\begin{bmatrix} 1 & x^T(0) \\ x(0) & X \end{bmatrix} \geq 0, \; \begin{bmatrix} X & M^T \\ M & \mu^2 \end{bmatrix} \geq 0, \forall i \in \{1, 2, \ldots, 16\}, \tag{16}$$

which are associated to a quadratic Lyapunov function $V(x) = x^T Px$, $P > 0$. Indeed, the first set (15) corresponds to a decay rate condition while the second set (16) guarantees $|u(t)| \leq \mu$ for a given initial condition $x(0)$ (Tanaka and Wang, 2001). The gain is recovered by $K = MX^{-1}$. There are several approaches for designing more complex stabilizing control laws, see for instance

(Bernal et al., 2011; Guerra et al., 2012; Márquez et al., 2016; González et al., 2016).

The aforementioned LMI approach allows obtaining a suitable gain K with sufficient "energy" to reach the reference while avoiding input saturation.

4.2 Trajectory tracking via dynamic regulation

Another way to face the problem of solving nonlinear partial differential equation (6)-(7) has been stated in (Robles and Bernal, 2015): it consists in finding a dynamical mapping $\pi(w)$ instead of a static one. This can be done for nonlinear setups of the form

$$\dot{x} = A(x)x + B(x)u \tag{17}$$

$$\dot{w} = S(w)w \tag{18}$$

$$e = Cx - Qw, \tag{19}$$

altogether with the nonlinear mappings $x = \pi(w) = \Pi(w)w$ and $u = \gamma(w) = \Gamma(w)w$. Hence, equations (6) and (7) yield

$$\dot{\Pi} = A(\Pi w)\Pi + B(\Pi w)\Gamma - \Pi S(w), \tag{20}$$

$$0 = C\Pi - Q, \tag{21}$$

where the arguments of $\Pi = \Pi(w)$ and $\Gamma = \Gamma(w)$ have been omitted. Let Π_{ij}, $\dot{\Pi}_{ij}$, and Γ_i being entries of their corresponding matrices Π, $\dot{\Pi}$, and Γ. Robles and Bernal (2015) proposed to solve (20)-(21) for Γ_i and Π_{ij} whenever an explicit solution is possible, and for $\dot{\Pi}_{ij}$ when no explicit solution of Π_{ij} can be computed.

5. SIMULATION AND REAL-TIME RESULTS

The control task is to design a controller such that the output $y(t) = x_3(t)$ is driven by $w_2(t)$, where the exosystem state is provided by

$$\dot{w}(t) = \underbrace{\begin{bmatrix} 0 & 8 \\ -8 & 0 \end{bmatrix}}_{S} w(t). \tag{22}$$

Therefore, we have $C = [0\ 0\ 1\ 0]$ and $Q = [0\ 1]$. Both the fuzzy approach and the dynamic one employ a single linear gain K computed via LMIs (15) and (16) with $\alpha = 0.4$, $\mu = 20$, $x(0) = [0\ 0\ 12^\circ\ 0]^T$, thus the obtained values are:

$$K = \begin{bmatrix} 1.519 \\ 3.664 \\ 89.641 \\ 12.705 \end{bmatrix}^T \text{ and } P = \begin{bmatrix} 0.012 & 0.023 & 0.413 & 0.073 \\ 0.023 & 0.056 & 0.979 & 0.174 \\ 0.413 & 0.979 & 22.068 & 3.226 \\ 0.072 & 0.174 & 3.226 & 0.555 \end{bmatrix}.$$

5.1 Via fuzzy regulation (Π_i, Γ_i)

In order to perform the task via the fuzzy TS models, the set of linear equations (14) produces 16 pairs of mappings (Π_i, Γ_i), for brevity only some of them are given below:

$$\Pi_1 = \begin{bmatrix} 0 & -9.465 \\ 75.723 & 0 \\ 0 & 1 \\ -8 & 0 \end{bmatrix}, \quad \Pi_5 = \begin{bmatrix} 0 & -5.403 \\ 43.223 & 0 \\ 0 & 1 \\ -8 & 0 \end{bmatrix},$$

$$\Pi_{11} = \begin{bmatrix} 0 & -6.639 \\ 53.115 & 0 \\ 0 & 1 \\ -8 & 0 \end{bmatrix}, \quad \Pi_{15} = \begin{bmatrix} 0 & -3.065 \\ 24.521 & 0 \\ 0 & 1 \\ -8 & 0 \end{bmatrix},$$

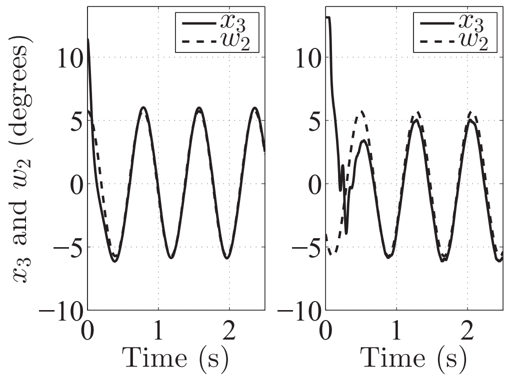

Fig. 2. Time evolution of $x_3(t)$ and $w_2(t)$: simulation (left) and real-time (right).

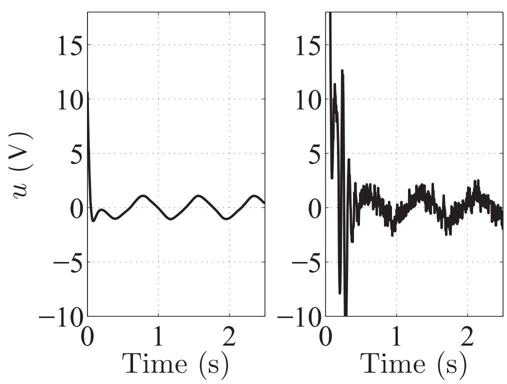

Fig. 3. Control signal $u(t)$: simulation (left) and real-time (right).

$\Gamma_1 = [0\ 16.271]$, $\Gamma_5 = [0\ 9.488]$, $\Gamma_{11} = [0\ 16.879]$, and $\Gamma_{15} = [0\ 10.096]$.

Simulation and real-time implementations are conducted for initial conditions $x(0) = [0\ 0\ 12^\circ\ 0]^T$ and $w(0) = [0\ 0.1]^T$. Fig. 2 displays the state $x_3(t)$ tracking the reference $w_2(t)$. In Fig. 3, it can be seen that control signal never surpasses the imposed limit 20V.

5.2 Via dynamic regulation

As stated before, solving (6) and (7) is a very difficult task. Instead, we first employ (21), the following has been found: $\Pi_{31} = 0$, $\Pi_{31} = -1$,$\Pi_{41} = 8$, $\Pi_{42} = 0$ and therefore $\dot{\Pi}_{31} = \dot{\Pi}_{32} = \dot{\Pi}_{41} = \dot{\Pi}_{42} = 0$. These values are substituted in (20), then, the remaining entries of $Pi(w)$, $\dot{\Pi}(w)$, and $\Gamma(w)$ can be computed:

$$\dot{\Pi}_{11} = \Pi_{21} + 8\Pi_{12}$$

$$\dot{\Pi}_{12} = \Pi_{22} - 8\Pi_{11}$$

$$\dot{\Pi}_{21} = 8\Pi_{22} + \frac{\Gamma_{11}(c_2 + c_3)}{\mu_2}$$

$$\dot{\Pi}_{22} = \frac{\Gamma_{12}(c_2 + c_3)}{\mu_2} - 8\Pi_{21} + \frac{\sin w_2 \left((c_2 + c_3)\mu_3 - c_4 \cos w_2 \mu_4\right)}{w_2 \mu_2}$$

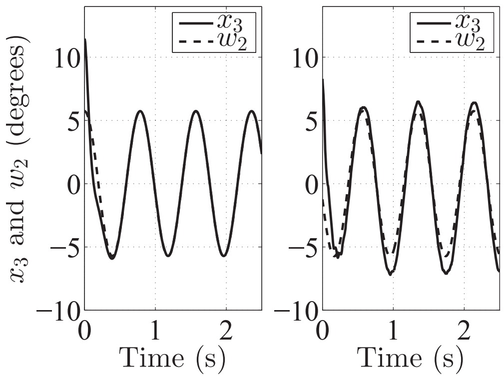

Fig. 4. State $x_3(t)$ and state $w_2(t)$ nonlinear regulation

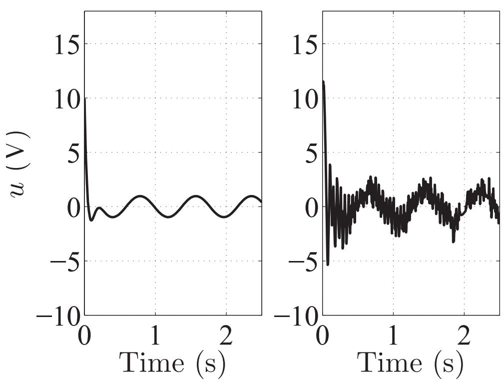

Fig. 5. Control law $u(t)$ nonlinear regulation

where

$$\begin{aligned}
\mu_1 &= \sin w_2 \left(\left(c_2 \sin^2 w_2 + c_1 \right) \mu_4 - c_4 \cos w_2 \mu_3 \right) \\
\mu_2 &= \left(c_2 + c_3 \right) \left(c_2 \sin^2 w_2 + c_1 \right) - c_4^2 \cos^2 w_2 \\
\mu_3 &= c_4 (\Pi_{42} w_2 + 8 w_1)^2 \\
&\quad -2 c_2 \cos w_2 \left(\Pi_{21} w_1 + \Pi_{22} w_2 \right) \left(\Pi_{42} w_2 - 8 w_1 \right) \\
\mu_4 &= \left(c_5 g + c_2 \cos w_2 (\Pi_{21} w_1 + \Pi_{22} w_2)^2 \right),
\end{aligned}$$

$\Gamma_{11} = 0$, and $\Gamma_{21} = \frac{1}{c_4 \cos w_2} \left(\mu_2 \left(\alpha_1 \alpha_2 + \frac{\mu_1}{w_2 \mu_2} \right) \right)$. And the mapping $\Gamma(w) = [\Gamma_{11} \;\; \Gamma_{12}]$.

Simulation as well as real-time have been performed for the very same initial conditions as the case above. In Fig. 4 shows $x_3(t)$ being driven by $w_2(t)$ while Fig. 5 plots the control signal. It can be seen that the trajectory tracking is performed better in the fuzzy case; however, the control law seems to be softer in the dynamic-mapping case. Worth noticing, the fuzzy case does not have a mathematical proof of being able to effectively perform output regulation, in contrast with the dynamic-mapping approach.

6. CONCLUSIONS

A real-time implementation of trajectory tracking on a Furuta pendulum has been presented. A comparison between two fuzzy schemes, namely fuzzy and dynamic regulation, have been done. It has become apparent that, despite its lack of mathematical proof, the fuzzy approach performed better on approximation basis. LMIs have been employed in both schemes in order to incorporate performance conditions.

REFERENCES

Begovich, O., Sanchez, E.N., and Maldonado, M. (2002). Takagi-Sugeno fuzzy scheme for real-time trajectory tracking of an underactuated robot. *IEEE Transactions on Control Systems Technology*, 10(1), 14–20.

Bernal, M., Soto-Cota, A., Cortez, J., Pitarch, J.L., and Jaadari, A. (2011). Local non-quadratic h-infinity control for continuous-time Takagi-Sugeno models. In *IEEE International Conference on Fuzzy Systems*, 1615–1620. Taipei, Taiwan.

Bernal, M., Marquez, R., Estrada-Manzo, V., and Castillo-Toledo, B. (2012). Nonlinear output regulation via Takagi-Sugeno fuzzy mappings: A full-information LMI approach. In *Fuzzy Systems (FUZZ-IEEE), 2012 IEEE International Conference on*, 1–7.

Fantoni, I. and Lozano, R. (2002). *Non-linear Control for Underactuated Mechanical Systems*. Communications and Control Engineering. Springer London, UK.

Francis, B. (1977). The linear multivariable regulator problem. *SIAM Journal of Control and Optimization*, 15, 486–505.

González, T., Bernal, M., Sala, A., and Aguiar, B. (2016). Cancellation-based nonquadratic controller design for nonlinear systems via Takagi-Sugeno models. *IEEE Transactions on Cybernetics*.

Guerra, T.M., Bernal, M., Guelton, K., and Labiod, S. (2012). Nonquadratic local stabilization for continuous-time Takagi-Sugeno models. *Fuzzy Sets and Systems*, 201, 40–54.

Isidori, A. (1995). *Nonlinear Control Systems*. Springer, London, 3 edition.

Isidori, A. and Byrnes, C.I. (1990). Output regulation of nonlinear systems. *IEEE Transactions on Automatic Control*, 35(2), 131–140.

Márquez, R., Guerra, T.M., Bernal, M., and Kruszewski, A. (2016). A non-quadratic Lyapunov functional for h control of nonlinear systems via Takagi–Sugeno models. *Journal of the Franklin Institute*, 353(4), 781–796.

Meda, J.A. and Castillo, B. (2009). Synchronization of chaotic systems from a fuzzy regulation approach. *Fuzzy Sets and Systems*, 160(19), 2860–2875.

Meda, J.A., Gomez, J.C., and Castillo, B. (2012). Exact output regulation for nonlinear systems described by Takagi-Sugeno fuzzy models. *IEEE Transactions on Fuzzy Systems*, 20(2), 235–247.

Quanser, I. (2006). *Mechatronics Control Kit User's Manual (Instructor)*. Mathworks, inc, Natick, MA.

Robles, R. and Bernal, M. (2015). Comments on exact output regulation for nonlinear systems described by Takagi-Sugeno fuzzy models. *IEEE Transactions on Fuzzy Systems*, 23(1), 230–233.

Tanaka, K. and Wang, H. (2001). *Fuzzy Control Systems Design and Analysis: A linear matrix inequality approach*. John Wiley & Sons, New York.

Taniguchi, T., Tanaka, K., and Wang, H. (2001). Model construction, rule reduction and robust compensation for generalized form of Takagi-Sugeno fuzzy systems. *IEEE Transactions on Fuzzy Systems*, 9(2), 525–537.